JOURNAL OF AGRICULTURAL AND FOOD CHEMISTRY

pubs.acs.org/JAFC
Article

Enhancement of Acarbose Production in *Actinoplanes* sp. QQ-12 via Multiple Engineering Strategies

Guoqiang Liu, Qi Liu, Xiaotong Song, Xingzhi Jiao, Wanping Zhou, Qianjin Kang, and Linquan Bai*

Cite This: *J. Agric. Food Chem.* 2025, 73, 12845−12855

ABSTRACT: The α-glucosidase inhibitor acarbose is used in the treatment of type 2 diabetes mellitus. Metabolic engineering is crucial to overcome acarbose production bottlenecks. Herein, a genetic toolkit was developed to enable metabolic engineering in *Actinoplanes* sp.. The attachment/integration (Att/Int) systems of ΦBT1, pSAM2, R4, and TG1 showed conjugation frequencies of 0.98−24.4%. Furthermore, three mutants were constructed by deleting nontarget biosynthetic gene clusters (BGCs) and inserting one to three additional copies of the acarbose biosynthetic gene cluster (*acb*). These mutants, with 2, 3, and 4 copies of *acb* gene cluster, demonstrated titer increases of 69.4%, 99.3%, and 24.2%, respectively, with a sharply declined titer in the four-copy *acb* strain LGQ-17::3*acb*. To rescue the acarbose titer in LGQ-17::3*acb*, we overexpressed rate-limiting genes *acbC*, *M*, *O*, *N*, *J*, *V*, *I*, or *S*. The overexpression of *acbJ* and *acbS* resulted in acarbose titer increases of 1.04-fold and 98%, respectively. Furthermore, following fed-batch fermentation optimization in shake flasks, the titer of acarbose in LGQ-17::3*acb*::*stnYp-acbJ* increased by 1.1-fold to reach 8.12 g/L. This genetic engineering toolkit with multiple Att/Int systems and high conjugation frequencies paves the way for future genetic engineering in *Actinoplanes* sp., and the engineered strain shows excellent potential for industrial application.

KEYWORDS: *acarbose production, Actinoplanes sp., genetic engineering, multiplex site-specific integration, fed-batch fermentation*

1. INTRODUCTION

Actinoplanes sp. SE50/110 (ATCC 31044) is the natural producer of acarbose (acarviosyl-1,4-maltose), an α-glucosidase inhibitor widely used in the treatment of type 2 diabetes mellitus since 1990.[1] T2DM has been on the rise globally, with more than 537 million adults (aged 20−79 years) suffering from the disease in 2021.[2] With the rapid global increase in the incidence of type 2 diabetes, the market demand for acarbose is expected to rise. In addition to reducing glucose absorption and improving postprandial blood sugar levels, acarbose has been shown to significantly reduce body weight, lower lipid levels, and improve insulin resistance by influencing gut microbiota metabolism. These additional effects highlight its potential as a health food ingredient.[3,4]

Although acarbose can be synthesized by several species of *Actinoplanes* and *Streptomyces*,[5,6] and its industrial production is mainly carried out via microbial fermentation using *Actinoplanes* sp. SE50/110-derived strains due to their higher acarbose production capacity.[1] In the early years, industrial acarbose production strains were developed exclusively through laborious, conventional mutagenesis and stepwise selection of overproducers.[7−11] While this high-yield strategy has proven effective, it is limited. In 2016, an *Escherichia coli-Actinoplanes* intergeneric conjugation system was developed to introduce actinophage-based integrative vectors for target gene overexpression, whereas gene knockout was achieved using the CRISPR/Cas9 system.[12,13] Around the same time, a more efficient genetic manipulation system was established using the mycelia of *Actinoplanes* sp., allowing for gene overexpression and inactivation via homologous recombination.[14] The establishment of these efficient conjugation transfer systems, along with multiomics analysis,[15,16] has facilitated the study of acarbose biosynthesis, regulation, and metabolism,[17−19] paving the way for yield improvement through metabolic engineering.

The acarbose biosynthetic gene cluster (*acb*) is 32.2 kb in length and contains 22 genes.[20] The basic acarbose biosynthetic pathway has been elucidated through biochemical experiments, isotope incorporation, and gene inactivation studies, which is valuable for making *Actinoplanes* sp. SE50/110 a more efficient acarbose biofactory through rational metabolic engineering.[21,22] Xie et al. identified two genes, *ACWT_4325* (encoding alcohol dehydrogenase) and *ACWT_7629* (encoding elongation factor G), by comparative genomics, which were the main factors contributing to the high yield of *Actinoplanes* sp. SE50/110 compared with the parental strain SE50.[23] Deletion of the *cgt* gene (coding for a highly expressed small carbohydrate-binding protein Cgt) in *Actinoplanes* sp. SE50/110 resulted in an acarbose titer increase of 8−16%.[24] Zhao et al. deleted *treY* (a maltooligosyltrehalose synthase gene), which led to a 10% increase in acarbose titer and eliminated the formation of the byproduct component C.[14] By diminishing shunt products and enhancing the supply of the amino-deoxyhexose moiety, acarbose production was increased by 1.2-fold, reaching 7.4 g/L.[21] A combination of strategies, including weakening the glycogen synthesis path-

Received: January 13, 2025
Revised: April 9, 2025
Accepted: April 30, 2025
Published: May 14, 2025

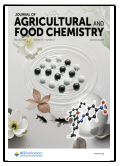

https://doi.org/10.1021/acs.jafc.5c00613
J. Agric. Food Chem. 2025, 73, 12845−12855

way, strengthening the glycogen degradation pathway, and fed-batch fermentation, increased the titer of acarbose by 58%, reaching 8.04 g/L.[25] These efforts have demonstrated the significant potential of rational metabolic engineering for increasing the acarbose titer.

Recently, overexpression of an entire biosynthetic gene cluster has been established as an effective method for enhancing the production of specific metabolites. This approach has been widely applied in several species, including *Escherichia coli*, *Saccharomyces cerevisiae*, *Bacillus subtilis*, and *Streptomyces*.[26−29] The goadsporin yield of engineered strains, which had one or two copies of the goadsporin BGC introduced, was increased by 1.46-fold and 2.25-fold compared with the wild-type strain, respectively.[30] Li et al. developed two strategies for multilocus chromosomal integration of BGCs, including multiplex site-specific genome engineering (MSGE) and advanced multiplex site-specific genome engineering (aMSGE).[31,32] Using MSGE, five copies of the pristinamycin II (PII) BGC were introduced into the genomes of *Streptomyces pristinaespiralis*, resulting in a 2.2-fold titer increase of pristinamycin.[31] Using aMSGE, up to four copies of 5-oxomilbemycin BGCs were introduced into *Streptomyces hygroscopicus*, resulting in a 1.9-fold titer increase of 5-oxomilbemycin.[32] Our group also found that inserting an *acb* gene cluster into the wild-type SE50/110 genome resulted in a 35% titer increase of acarbose.[14] Therefore, we anticipate that combining the multicopy gene cluster strategy in a good chassis strain will improve the acarbose titer and break the existing titer bottleneck.

Herein, we first systematically developed a genetic modification toolkit. Then, to insert different copies of *acb*, chassis strains harboring multicopy $attB^{\Phi C31}$[31] were generated. Subsequently, one to three copies of *acb* were integrated into the chromosome of various *Actinoplanes* sp. chassis strains in a single step. However, we found that the acarbose titer of the strain with four copies of *acb* sharply decreased compared with the strain with three copies of *acb*. Overexpressing rate-limiting enzymes restored a high acarbose titer in the strain with four copies of *acb*. Finally, acarbose production was further enhanced through fed-batch fermentation optimization.

2. MATERIALS AND METHODS

2.1. Plasmids, Strains, Culture Conditions, and General Techniques. Plasmids and strains used in this study are listed in Table S1.

E. coli DH10B was used for DNA cloning, and ET12567-(pUZ8002) was used for the intergeneric conjugation between *E. coli* and the mycelia of *Actinoplanes* sp.. *E. coli* strains were grown at 37 °C in Luria−Bertani (LB) medium or on LB agar plates. *Actinoplanes* sp. SE50/110 and its derivatives were cultivated on STY agar medium (g/L, sucrose 30 g, tryptone 5 g, yeast extract 5 g, casein hydrolysate 1 g, $K_2HPO_4{\cdot}3H_2O$ 1 g, KCl 0.5 g, $FeSO_4$ 0.05 g, agar 20 g, pH 7.2) at 30 °C for 2−4 days and then inoculated into 30 mL of SM medium (g/L, maltose 10 g, glucose 15 g, glycerol 10 g, malt extract 10 g, yeast extract 5 g, tryptone 5 g, casein hydrolysate 1 g, $K_2HPO_4{\cdot}3H_2O$ 1 g, pH 7.2) in a 250 mL baffled flask for 32−36 h on a rotary shaker (30 °C, 220 rpm) for fermentation or genomic DNA extraction. The seed medium contained 4% soya flour, 1.5% maltose, 1% glucose, 1% soluble starch, 1% glycerol, and 0.2% $CaCO_3$ (pH 7.2, 115 °C, 30 min for autoclave sterilization). The fermentation medium contained 5% maltose, 3% glucose, 1% soya flour, 0.4% yeast, 0.3% glutamate, 0.25% $CaCO_3$, 0.1% $K_2HPO_4{\cdot}3H_2O$, and 0.05% $FeCl_3$ (pH 7.2, 115 °C, 30 min for autoclave sterilization). Antibiotics (final concentrations of 50 mg/L for kanamycin and apramycin and 25 mg/L for chloramphenicol) were added when necessary.

Oligonucleotide primer synthesis and sequencing of PCR-amplified products were performed by Tsingke Biological Technology or Sangon Biotech (Shanghai) Co., Ltd. DNA polymerase was purchased from Nanjing Vazyme Biotech Co., Ltd. T4 DNA ligase was purchased from Takara. The NovoRec Plus One-Step PCR Cloning Kit was used to construct vectors using a homologous recombination method (Novoprotein). An E.Z.N.A. Gel Extraction Kit (Omega Bio-Tek) was used to purify the PCR products. An E.Z.N.A. BAC/PAC DNA Kit (Omega Bio-Tek) was used to isolate fosmid pLQ666. 5-Flucytosine was purchased from Adamas. Antibiotics were purchased from Beijing Lablead Biotech Co., Ltd. and Inalco Spa, Milano, Italy. Other biochemicals were purchased from Sangon Biotech, Sigma-Aldrich, Sinopharm Chemical Reagent Co., Ltd., or Oxoid.

2.2. Construction of the Vector pRT801-*str*. The streptomycin resistance gene, *SmR*, was amplified by PCR using pIJ778 as the template DNA and primers *str*-F/R. A fragment with 43-bp homologous sequences at both ends was amplified by PCR using the *SmR* fragment as the template DNA and primers Target-801-*str*-F/R. The fragment and plasmid pRT801 were subsequently transformed into GB08-*red* by PCR targeting to generate pRT801-*str*.[33] The primers and oligonucleotide sequences used in this study are provided in Table S2.

2.3. Construction of Gene Knockout Mutants. To delete the gene *treY*, pLQ756 was transferred to ET12567-(pUZ8002) and then introduced into QQ-12 by intergeneric conjugation. The intergeneric conjugation was performed as described previously.[14] The exconjugants were selected, cultured, and verified by PCR using primers del-*treY*-F/R. The mutant LGQ-4, bearing a native $attB^{\Phi C31}$ site, gave a 0.73 kb amplified fragment, whereas the parental strain QQ-12 yielded a 1.80 kb amplified fragment (Figure S5).

To delete Region 10 (from *ACPL_4110* to *ACPL_4123*, 27.8 kb) and introduce an artificial $attB^{\Phi C31}$ site in mutant LGQ-4, upstream and downstream homologous arms were obtained by PCR amplification using the genomic DNA of LGQ-4 as the template and primer pairs *RE10*-up-F/R and *RE10*-dw-F/R, respectively, and then cloned into *Bam*HI/*Hin*dIII-digested plasmid pLQ752 to generate pLQ1962. The pLQ1962 was transferred to ET12567(pUZ8002) and subsequently introduced into LGQ-4 by intergeneric conjugation. The exconjugants were selected, cultured, and verified by PCR amplification using primers *RE10*-YZ-F/R. The mutant LGQ-14, with two $attB^{\Phi C31}$ sites (a native one and an artificial one), gave a 0.61 kb amplified fragment, whereas the parental strain LGQ-4 had no amplified product (Figure S8). Similarly, using LGQ-4 as the parental strain, mutants LGQ-12, LGQ-13, LGQ-15, and LGQ-16 were constructed with deletions of essential genes in Regions 2, 6, 14, and 20, respectively (Figures S6−S10).

In order to obtain a strain containing three $attB^{\Phi C31}$ sites, Region 2 was deleted in LGQ-14 (Figure S11). The mutant LGQ-17 carried deletions in Regions 2 and 10 and three $attB^{\Phi C31}$ sites (one native and two artificial ones). Furthermore, the corresponding PCR products for all mutants were verified by DNA sequencing.

https://doi.org/10.1021/acs.jafc.5c00613
J. Agric. Food Chem. 2025, 73, 12845−12855

2.4. Construction of *Actinoplanes* sp. Mutants with Multicopy *acb* Gene Clusters. To introduce an extra copy of the *acb* gene cluster, a fosmid pLQ666 carrying the entire *acb* gene cluster was transferred to ET12567(pUZ8002) and subsequently introduced into LGQ-4 (containing a native $attB^{\Phi C31}$ site) by conjugation. The exconjugants of the engineered strain LGQ-4::*acb* were selected, cultured, and verified by PCR amplification using primers *attB*-R-F/-R. The correct exconjugants gave a 1.0 kb amplified product (Figure S12). The validated primers contained one located in the genome and the other in pLQ666[29]. Similarly, LGQ-4::pSET152 was constructed as a control strain using the vector plasmid pSET152.

To introduce two extra copies of the *acb* gene cluster, pLQ666 was transferred into ET12567(pUZ8002) and subsequently introduced into LGQ-14 with two $attB^{\Phi C31}$ sites by conjugation. The exconjugants of the engineered strain LGQ-14::2*acb* were selected, cultured, and verified by PCR using primers *attB*-R-F/R and *Re10*-L-F/*SCO*-L-R. The correct exconjugants gave ∼1.0 kb and ∼1.01 kb amplified products, respectively (Figure S12). Similarly, LGQ-14::2pSET152 was constructed as a control strain using the vector plasmid pSET152.

To introduce three extra copies of the *acb* gene cluster, pLQ666 was transferred into ET12567(pUZ8002) and subsequently introduced into LGQ-17 with three $attB^{\Phi C31}$ sites by conjugation. The exconjugants of the engineered strain LGQ-17::3*acb* were selected, cultured, and verified by PCR. The primer pairs *attB*-R-F/R, *Re10*-L-F/*SCO*-L-R and *Re2*-L-F/*SCO*-L-R were used to track the integration of pLQ666 into the corresponding $attB^{\Phi C31}$sites, and the correct exconjugants gave ∼1.0 kb, ∼1.01 kb, and ∼0.88 kb amplified products, respectively (Figure S12). Similarly, LGQ-17::3pSET152 was constructed as the control strain using vector plasmid pSET152.

2.5. Construction of pRT801-*str*-Derived Integrative Plasmids and Corresponding Engineered Strains. To overexpress rate-limiting genes in LGQ17::3*acb*, we constructed a plasmid, pRT801-*str* (Figure S13). Using the plasmid pSET152-*kasOp*-acbJ* as the template, the *kasOp** promoter fragment was obtained by PCR amplification with primers *kasOp*-801-Gib-up-F/R. Using the genomic DNA of *Actinoplanes* sp. QQ-12 as the template, the gene *acbC* was obtained by PCR amplification with primers *kasOp-C*-Gib-dw-F/R. Then, these two DNA fragments were assembled by overlap PCR using primers *kasOp*-801-Gib-up-F/*kasOp-C*-Gib-dw-R. The assembled DNA fragment was cloned into *Bcu*I/*Bam*HI-digested pRT801-*str* using a one-step cloning kit (Novoprotein) to yield pRT801-*str-kasOp*-acbC*.

Fragments containing *acbM, O, N, S, V, I*, or *J* were obtained by PCR amplification using the genomic DNA of *Actinoplanes* sp. QQ-12 as the template with the corresponding primers. Similarly, pRT801-*str-kasOp*-acbM,* pRT801-*str-kasOp*-acbO,* pRT801-*str-kasOp*-acbN,* pRT801-*str-kasOp*-acbS,* pRT801-*str-kasOp*-acbV,* pRT801-*str-kasOp*-acbI,* and pRT801-*str-kasOp*-acbJ* were constructed. Using pSET152-*ermEp*-acbJ* and pSET-*stnYp-indC* as the templates, the fragments *ermEp-acbJ* and *stnYp-acbJ* were obtained by PCR amplification with primers *ermEp-J*-Gib-F/R and *stnYp-J*-Gib-up-F/R, respectively. The resulting DNA fragments were cloned into *Bcu*I/*Bam*HI-digested pRT801-*str* using the one-step cloning kit to yield pRT801-*str-ermEp*-acbJ* and pRT801-*str-stnYp-acbJ*, respectively.

The pRT801-*str* and recombinant plasmids were transferred into ET12567(pUZ8002) and then introduced into LGQ17::3*acb* by intergeneric conjugation. The correct exconjugants were verified by PCR using primers 801-*str*-YZ-F/801-*str-C*-YZ-R, 801-*str*-YZ-F/801-*str-M*-YZ-R, 801-*str*-YZ-F/801-*str-O*-YZ-R, 801-*str*-YZ-F/R, 801-*str*-YZ-F/801-*str-J*-YZ-R, 801-*str*-YZ-F/801-*str-S*-YZ-R, 801-*str*-YZ-F/801-*str-V*-YZ-R, 801-*str*-YZ-F/801-*str-I*-YZ-R, 801-*str*-YZ-F/801-*str-J*-YZ-R, or 801-*str*-YZ-F/801-*str-J*-YZ-R, yielding the mutants LGQ-17::3*acb*::*kasOp*-acbC, -M, -O, -N, -J, -S, -V, -I, ermEp*-acbJ* or *stnYp-acbJ*. LGQ-17::3*acb*::pRT801-*str* was constructed as a control strain. The verification of the plasmids and mutants by PCR is shown in Figure S14.

2.6. Acarbose Fermentation of *Actinoplanes* sp. Strains. To assess the acarbose titer and biomass of *Actinoplanes* sp. mutants, 4 mL of SM culture was transferred to 40 mL of seed medium (in a 250 mL baffled flask) and cultivated for 30−32 h on a rotary shaker (30 °C, 220 rpm). Then, 7.5 mL of seed culture was inoculated to 50 mL of fermentation medium (in a 250 mL baffled flask) and cultivated for 4 days. Furthermore, 1 g of glucose was supplemented to each flask on day 2. Finally, the acarbose titer and the biomass (dry cell weight) were measured after the 4-day fermentation.

For the engineered strain LGQ-17::3*acb*::*stnYp-acbJ*, STY solid plate incubation time was 5 days, SM liquid medium incubation time was 32−33 h, and seed incubation time was 34−36 h. Seed inoculation was 15%, and the pH of the fermentation medium was 7.0−7.2. And 1% glucose and 0.67% maltose were added supplementally every day from 1 to 5 days in a baffled flask and a 3 L bioreactor. The fermentation lasted for 8 days, with samples taken every 24 h. In particular, for the 3 L bioreactor, dissolved oxygen was maintained at 30%, pH was not controlled, and the stirring speed was correlated with dissolved oxygen.

2.7. HPLC Analysis of the Titer of Acarbose and Shunt Products 1-*epi*-Valienol and Valienol. The supernatant of the fermentation broth was obtained by centrifugation at 12,000 rpm for 10 min and diluted 5-fold. The supernatant was directly analyzed for the accumulation of acarbose and shunt products (1-*epi*-valienol and valienol) using HPLC (Agilent Series 1260, Agilent Technologies, USA) with an Agilent ZORBAX NH_2 column (4.6 × 250 mm^2, particle size 5 μm). The elution buffer consisted of acetonitrile/phosphate (65:35, v/v) at a flow rate of 1 mL/min, and detection was performed at 210 nm. Then, the titer of acarbose was calculated according to a standard curve of acarbose and processed using Origin 9.8 software.

Similarly, the total accumulation of 1-*epi*-valienol/valienol was detected and calculated according to a standard curve of mixed 1-*epi*-valienol and valienol.[21] Each experiment included at least three independent biological replicates, with error bars representing the standard deviations. Two-tailed paired *t* tests were used for statistical analysis. The *p* values were obtained by comparing the control groups with the corresponding experimental groups, $p < 0.05$, $p < 0.01$, and $p < 0.001$ were defined as significant, moderately significant, and highly significant, respectively. Statistical analyses were performed using SPSS 29.0 (Statistical Product and Service Solutions) software.

2.8. Analysis of Biomass. To analyze the biomass of *Actinoplanes* sp. mutants, mycelia from 1 mL of culture were collected by centrifugation, washed with 0.5 M hydrochloric

https://doi.org/10.1021/acs.jafc.5c00613
J. Agric. Food Chem. 2025, 73, 12845−12855

Table 1. Conjugation Frequency of Different *AttB* Sites in *Actinoplanes* sp.[a]

AttB	Plasmid	Quantity of donor cells (CFU)	Quantity of recipient cells (CFU)	Quantity of exconjugants (CFU)	Conjugation frequency[b]	Integration sites
ΦBT1	pRT801	$9-11 \times 10^4$	1.6×10^3	181 ± 19	$11.3 \pm 1.19\times10^{-2}$	/
pSAM2	ppM927-*xis*			156 ± 11	$9.8 \pm 0.69\times10^{-2}$	/
R4	pLR4			390 ± 110	$24.4 \pm 6.88\times10^{-2}$	*ACPL_4548*
TG1	pLTG1			6 ± 3	$0.38 \pm 0.19\times10^{-2}$	*ACPL_836*

[a]QQ-2. [b]Values represent average frequencies from three independent experiments.

acid, centrifuged at 12,000 rpm for 10 min, and then dried at 65 °C in an oven until a constant weight was reached. The dry cell weight was measured with a precision balancer. Each experiment had at least three independent biological replicates, with error bars showing the standard deviations. The standard deviations and two-tailed paired *t* tests were used for statistical analysis.

2.9. RNA Extraction and Quantitative Real-Time PCR (qRT-PCR) Analysis. The expression of each gene during acarbose production was measured by qRT-PCR. Mycelia were collected from 1 mL of 48 h fermentation culture by centrifuging at 4 °C, frozen in liquid nitrogen for 0.5 h, and then stored at −80 °C. RNA extraction and qRT-PCR analysis were performed as previously described.[21] Primers used are listed in Table S2. The relative transcription values of target genes were calculated by the $2^{-\Delta\Delta Ct}$ method with the housekeeping gene *hrdB* (*ACPL_1268*) as an internal control. qRT-PCR analysis was performed in triplicate for each gene and repeated with three independent RNA samples, and error bars represent the standard deviations.

2.10. Detection of Endogenous 1-*epi*-Valienol-7-P and Valienol-7-P. Two samples, 1 mL each, were obtained from the 2-day fermentation culture by centrifugation. One sample was dried, and the biomass was measured. The other was washed twice with cold 0.9% NaCl, resuspended in ddH_2O, lysed by sonication, and quickly mixed with 1 mL of cold methanol. The supernatant was collected by centrifugation at 12,000 rpm for 10 min and freeze-dried. The lyophilized powder was resuspended in 100 μL of methanol/water solution (50:50, v/v), centrifuged at 12,000 rpm for 10 min, and analyzed by HPLC-QQQ/MS. The total amount of 1-*epi*-valienol-7-P and valienol-7-P was calculated according to the corresponding biomass. The total amount of 1-*epi*-valienol-7-P and valienol-7-P in SE50/110::pSET152 was set to 1, and those of the mutants were accordingly calculated.

3. RESULTS

3.1. Development of Genetic Engineering Toolkit for *Actinoplanes* sp. Site-specific recombination (SSR), based on Att/Int systems, has been widely exploited for stable chromosomal integration of target genes.[34] Several site-specific integration systems have been characterized and used as integrated vectors to enhance the production of many BGCs in actinobacteria, including ΦC31, ΦBT1, VWB, TG1, R4, ΦJoe, μ1/6, and pSAM2.[28,32] Four Att/Int systems—ΦBT1, pSAM2, R4, and TG1—were selected to verify their abilities and efficiencies in mediating SSR between *E. coli* ET12567-(pUZ8002) carrying the integrative plasmid and the mycelia of *Actinoplanes* sp. As shown in Table 1, the integrative vectors pRT801 ($attP^{\Phi BT1}$), ppM927-*xis* ($attP^{pSAM2}$), pLR4 ($attP^{R4}$), and pTG1 ($attP^{TG1}$) showed conjugation frequencies of $11.3 \pm 1.19 \times 10^{-2}$ (~11.3%), $9.8 \pm 0.69 \times 10^{-2}$ (~9.8%), $24.4 \pm 6.88 \times 10^{-2}$ (~24.4%) and $0.38 \pm 0.19 \times 10^{-2}$ (~0.98%), respectively. This indicates that ΦBT1, pSAM2, R4, and TG1 can efficiently mediate the insertion of exogenous DNA fragments into the *Actinoplanes* sp. genome.

To determine the insertion location of the integrated plasmid for the Att/Int system in the genome, homologous alignments were performed for the above-mentioned four integration systems and the genome of SE50/110 using SnapGene 6.0.2 software. Sequence consistency analysis between the candidate *attB* and *attP* sites was then performed using DNAMAN 6.0.3 software. According to the sequence alignments, the sequence consistency of R4 and TG1 exceeded 70% (Table S3). Subsequently, the possible integration sites of pLR4 and pTG1 in the *Actinoplanes* sp. QQ-2 genome were tested by PCR and sequencing. As shown in Figures S1,S2 and Table 1, the $attB^{R4}$ site was located within the gene *ACPL_4548* (an aminotransferase-coding gene) using two pairs of primers, R4-YZ-F/R and R4-4548-YZ-F/R, and the $attB^{TG1}$ site was located within the gene *ACPL_836* (an AMP-binding domain protein-coding gene) using two pairs of primers, TG1-YZ-F/R and TG1-836-YZ-F/R. However, ΦBT1 and pSAM2 showed no similar sequences when aligned with the genome. It was previously reported that the integrated vector pRT801 was inserted into an intergenic space (between genes *ACPL_7730* and *ACPL_7731*). Interestingly, we found that pRT801 was inserted into the genome of *Actinoplanes* sp. QQ-2 using the primers BT1-YZ-F/R, but not in the intergenic space when using the primers BT1-*7730*-YZ-F/R, as verified by PCR (Figure S3). Therefore, through homologous sequence alignment and PCR verification, it is possible to assess the integration positions quickly and accurately in specific strains.

Subsequently, the effects of site-specific recombination mediated by the Att/Int systems on the acarbose titer and biomass of *Actinoplanes* sp. were tested. Plasmids pRT801, ppM927-*xis*, pLR4, and pLTG1 were introduced into QQ-2 by intergeneric conjugation to generate the corresponding engineered strains. As shown in Figure 1, there were no significant differences in the acarbose titer or dry cell weight of QQ-2::pRT801, QQ-2::ppM927-*xis*, QQ-2::pLR4, and QQ-2::pLTG1 compared with the parental strain QQ-2, indicating the validity of the insertions of these four integrative vectors. However, compared with the control strain QQ-2, the acarbose titer and dry cell weight of QQ-2::pSET152 were decreased by 21.9% and 10.2%, respectively.

Apramycin has been proven to be a reliable antibiotic selection marker for the conjugation of *Actinoplanes* sp.,[21,25] but it does not meet the requirements for iterative metabolic engineering modifications. To implement multiple engineering strategies in *Actinoplanes* sp., it is necessary to determine the antibiotic resistance spectra of *Actinoplanes* sp. for the selection of resistance genes for plasmid construction. We found that *Actinoplanes* sp. was also sensitive to streptomycin, spectinomycin, and hygromycin. The optimal final concentrations for streptomycin, spectinomycin, and hygromycin were deter-

https://doi.org/10.1021/acs.jafc.5c00613
J. Agric. Food Chem. 2025, 73, 12845−12855

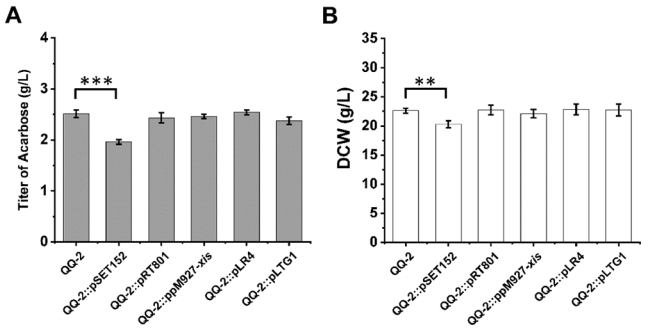

Figure 1. The effect of site-specific integration systems on the titer of acarbose and dry cell weight in *Actinoplanes* sp.. Acarbose titer (A) and dry cell weight (B) of QQ-2::pSET152 (harboring $attB^{\Phi C31}$), QQ-2::pRT801 (harboring $attB^{\Phi BT1}$), QQ-2::ppM927-*xis* (harboring $attB^{pSAM2}$), QQ-2::pLR4 (harboring $attB^{R4}$), QQ-2::pLTG1 (harboring $attB^{TG1}$), and QQ-2 (as a control). Error bars, mean ± SD (n = 3 biological replicates). ***, $p < 0.001$.

mined to be 0.1, 50, and 10 mg/L, respectively (Tables S4 and S5). Therefore, the resistance genes for streptomycin, spectinomycin, and hygromycin were chosen as selection markers for plasmid construction.

3.2. Constructions of Chassis Strains for Inserting Multicopy *acb* Gene Clusters. Using QQ-12, a high-yield mutant with reduced accumulation of shunt products,[21] as the parental strain, the maltooligosyltrehalose synthase gene *treY*, responsible for the synthesis of component C,[14] was deleted in frame to construct a mutant LGQ-4 (QQ-12Δ*treY*) (Figure S5), which contained the native $attB^{\Phi C31}$ site, allowing for the integration of one copy of *acb* gene cluster. As shown in Figure 2C, the acarbose tier of the engineered strain LGQ-4 increased by 9% compared with that of the parental strain QQ-12.

Based on antiSMASH analysis,[35] we found that the *Actinoplanes* sp. genome harbored 20 BGC regions with the capacity to produce various secondary metabolites, such as acarbose, nonribosomal peptides (NRPs), polyketides (PKS), terpenes, and melanin (Figure 2A). Among them, the *acb* gene cluster is located in Region 8, and the native $attB^{\Phi C31}$ site is located between Region 17 and Region 18, which allows overexpression of target genes through the ΦC31 Att/int system.

To knock out nontarget BGC regions and introduce several artificial $attB^{\Phi C31}$ integration sites, the transcription of different regions was analyzed based on the *Actinoplanes* sp. SE50/110 transcriptomes at different time points: day 1 (1D), day 2 (2D), and day 3 (3D).[21] Four regions (Regions 2, 6, 10, and 20) with high transcription were identified as candidate insertion locations for artificial $attB^{\Phi C31}$ (Figure 2B). To integrate more *acb* gene clusters, Region 14 was selected to ensure that the *attB* site insertions are discretely distributed on the chromosome. We deleted nontarget Regions 2 (~82.8 kb),6 (~14.3 kb),10 (~27.8 kb),14 (~30.9 kb), and 20 (~16.2 kb) and simultaneously inserted an artificial $attB^{\Phi C31}$ (originating from *S. coelicolor*, *Sco*) into the LGQ-4 chromosome via homologous recombination. The resulting strains were named LGQ-12 (Region 2 deletion), LGQ-13 (Region 6 deletion), LGQ-14 (Region 10 deletion), LGQ-15 (Region 14 deletion), and LGQ-16 (Region 20 deletion), and they were verified by PCR amplification and DNA sequencing (Figures S6–S10).

Fermentation analysis showed that the mutants LGQ-12 and LGQ-14 exhibited an increase in acarbose titer by 10.5% and

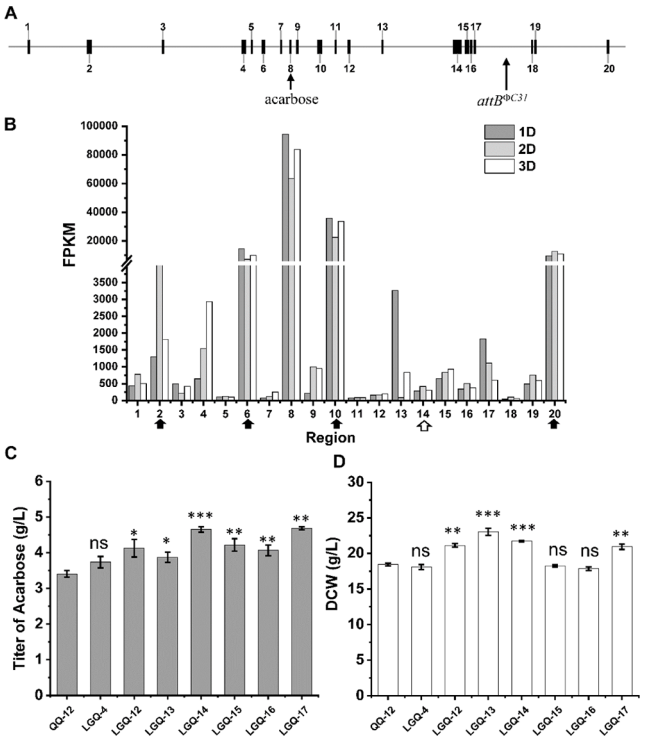

Figure 2. Knockout of nontarget BGC regions in *Actinoplanes* sp. and the construction of chassis strains. (A) Genomic distribution of BGC regions in *Actinoplanes* sp. SE50/110 analyzed by antiSMASH. The numbers of 1–20 represent BGC regions predicted by antiSMASH. The locations of *acb* and $attB^{\Phi C31}$ site are marked. (B) Relative transcription of BGC regions in *Actinoplanes* sp. SE50/110. Thick black arrows: active BGC regions, hollow white arrow: a candidate BGC region to guarantee multiple *attB*s discrete distributions; Acarbose titer (C) and dry cell weight (D) of LGQ-4 (QQ-12Δ*treY*), LGQ-12 (LGQ-4ΔRegion 2::$attB^{\Phi C31}$), LGQ-13 (LGQ-4ΔRegion 6::$attB^{\Phi C31}$), LGQ-14 (LGQ-4ΔRegion 10::$attB^{\Phi C31}$), LGQ-15 (LGQ-4ΔRegion 14::$attB^{\Phi C31}$), LGQ-16 (LGQ-4ΔRegion 20::$attB^{\Phi C31}$), LGQ-17 (LGQ-14ΔRegion 2::2$attB^{\Phi C31}$), and QQ-12 (as a control strain). Error bars, mean ± SD (n = 3 biological replicates). ns, no significant, *, $p < 0.05$, **, $p < 0.01$, and ***, $p < 0.001$.

24.3%, respectively, compared with the parental strain LGQ-4 (Figure 2C), as well as a respective increase in dry cell weight (DCW) by 16.9% and 20.2% (Figure 2D). The mutants LGQ-15 and LGQ-16 showed increases in acarbose titer by 12.7% and 8.6%, respectively, but had no significant effect on biomass compared to LGQ-4. In contrast, LGQ-13 had no significant effect on acarbose production and biomass when compared with LGQ-4.

To develop a chassis strain capable of integrating multicopy *acb* gene clusters, another artificial $attB^{\Phi C31}$ site was introduced by replacing Region 2 in the genome of LGQ-14. Accordingly, we deleted Region 2 in LGQ-14 to obtain the mutant LGQ-17, which contains three $attB^{\Phi C31}$ sites (a native one and two artificial ones), and it was verified by PCR amplification and DNA sequencing (Figure S11). However, compared with the parental strain LGQ-14, LGQ-17 showed no significant improvement in acarbose titer and biomass (Figure 2C,D). Thus, we obtained three chassis strains capable of integrating one to three extra copies of the *acb* gene clusters in *Actinoplanes* sp..

https://doi.org/10.1021/acs.jafc.5c00613
J. Agric. Food Chem. 2025, 73, 12845–12855

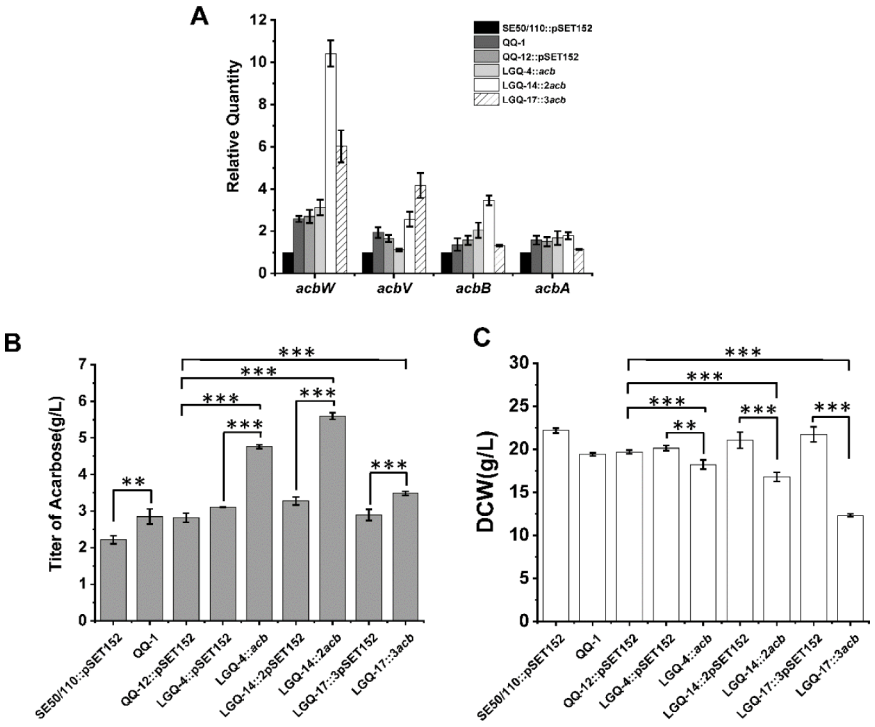

Figure 3. Enhanced acarbose production by multicopy acarbose gene clusters strategy. (A) Transcriptional analysis of *acbW*, *acbV*, *acbB*, and *acbA* in engineered strains with one to four copies of the *acbs* at 48 h during the fermentation process by quantitative real-time PCR. With the housekeeping gene *hrdB* as an internal control, the relative transcription of the tested genes was calculated by the $2^{-\Delta\Delta Ct}$ method. The average transcription of tested genes for SE50/110::pSET152 were set to 1 as standard, and gene expression of other engineered strains was calculated accordingly. Acarbose titer (B) and dry cell weight (C) of engineered strains with one to four copies of the *acbs*. LGQ-4::*acb* has 2*acb* (LGQ-4::pSET152 as a control), LGQ-14::2*acb* has 3*acb* (LGQ-14::2pSET152 as a control), and LGQ-17::3*acb* has 4*acb* (LGQ-17::3pSET152 as a control). Error bars, mean ± SD (n = 3 biological replicates). *, $p < 0.05$; **, $p < 0.01$; and ***, $p < 0.001$.

3.3. Introducing Multicopy *acb* Gene Clusters to Enhance Acarbose Production in *Actinoplanes* sp. To enhance acarbose production, pLQ666, with a cloned entire *acb* gene cluster, was transferred to the chassis strains LGQ-4, LGQ-14, or LGQ-17, resulting in the construction of a two-copy *acb* strain, LGQ-4::*acb*, a three-copy *acb* strain, LGQ-14::2*acb*, and a four-copy *acb* strain, LGQ-17::3*acb* via conjugal transfer.

In *Actinoplanes* sp., the native $attB^{\Phi C31}$ is located within gene *ACPL_6602*[12], and the insertion locations of the two artificial $attB^{\Phi C31}$ sites (*RE10 attB* and *RE2 attB*) in the genome were designed to facilitate the accurate identification of multicopy *acbs* mutants by PCR. According to the integration principle of $attB^{\Phi C31}$,[29] we designed a primer pair specific for the three $attB^{\Phi C31}$ sites, with one primer located in pLQ666 and the other in the genome, to obtain specific amplified DNA fragments through PCR. The exconjugants of the engineered strain LGQ-4::*acb* were verified by PCR using primers *attB*-R-F/R (Figure S12A). Similarly, using the integrative vector plasmid pSET152, LGQ-4::pSET152 was constructed as the control strain and verified by PCR using primers *attB*-R-F/R. The exconjugants of the engineered strain LGQ-14::2*acb* and the control strain LGQ-14::2pSET152 were verified by PCR using primers *attB*-R-F/R and *Re10*-L-F/*SCO*-L-R (Figure S12B). The exconjugants of the engineered strain LGQ-17::3*acb* and the control strain LGQ-17::3pSET152 were verified by PCR using primers *attB*-R-F/R, *Re10*-L-F/*SCO*-L-R, and *Re2*-L-F/*SCO*-L-R (Figure S12C).

Fermentation analysis showed that the integration of QQ-1 increased the acarbose titer by 29.0% compared with the wild-type SE50/110::pSET152 (Figure 3B), which is consistent with a previous report.[14] Additionally, LGQ-4::*acb* increased the acarbose titer by 53.1% compared to LGQ-4::pSET152, indicating that QQ-12 is an excellent chassis strain. The acarbose titer of LGQ-14::2*acb*, with two extra copies of *acb*, reached approximately 5.6 g/L, representing a 71.3% improvement over that of LGQ-14::2pSET152. However, the integration of three extra copies of *acb* in strain LGQ-17::3*acb* showed only a 20.3% increase in acarbose titer compared with LGQ-17::3pSET152. The significant decrease in strain LGQ-17::3*acb* compared with LGQ-14::2*acb* suggests that further addition of *acb* would not contribute to an increase in acarbose titer. When compared with the starting control strain QQ-12::pSET152, the strains LGQ-4::*acb*, LGQ-14::2*acb*, and LGQ-17::3*acb* showed a 69.4%, 99.3%, and 24.2% increase in acarbose titer (Figure 3B), respectively, but a 7.6%, 14.7%, and 37.6% decrease in biomass (Figure 3C). Meanwhile, the transcription of *acbW*, *acbV*, *acbB*, and *acbA* involved in acarbose biosynthesis in LGQ-4::*acb*, LGQ-14::2*acb*, and LGQ-17::3*acb* have different degrees of improvement, up to 2.85-fold compared with QQ-12::pSET152 (Figure 3A). These results indicate that increasing the copy numbers of *acb* enhanced the transcription of acarbose biosynthetic genes, thereby dramatically improving the yield of acarbose.

3.4. Mining the Rate-Limiting Enzymes of the Four-Copy *acbs* Strain LGQ-17::3*acb* to Invert Acarbose Production Capacity. The productivity (ratio of titer and dry cell weight, g/g) of the three-copy *acb* strain LGQ-14::2*acb* and the four-copy *acb* strain LGQ-17::3*acb* is 0.33 and 0.28,

https://doi.org/10.1021/acs.jafc.5c00613
J. Agric. Food Chem. 2025, 73, 12845−12855

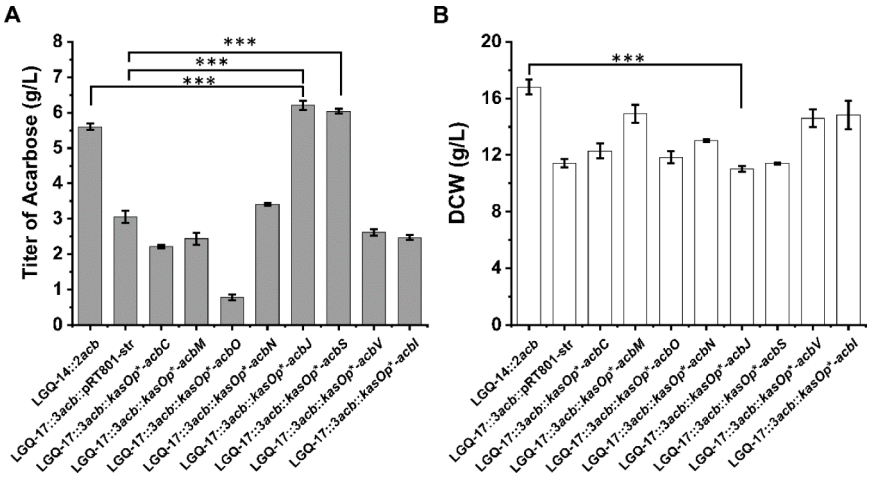

Figure 4. Mining rate-limiting enzyme of acarbose biosynthesis in LGQ-17::3*acb* with four-copy *acb*s. Acarbose titer (A) and dry cell weight (B) of LGQ-17::3*acb* with four-copy *acbs* overexpressing the rate-limiting factor. The candidate genes *acbC, M, O, N, J, S, V, I* were expressed under the control of *kasOp** promoter. The LGQ-17::3*acb*::pRT801-*str* was constructed as a control strain. Streptomycin was used to screen exconjugants. Error bars, mean ± SD (n = 3 biological replicates). ***, $p < 0.001$.

respectively. The acarbose production capacity of LGQ-17::3*acb* is lower than that of LGQ-14::2*acb*, which is inconsistent with our expectations. The biosynthetic pathways of secondary metabolites involve the synergistic action of multiple enzymes and enhancing the catalytic ability of rate-limiting enzymes can greatly increase the yield of natural products in actinobacteria.[26,36] We speculated that the presence of rate-limiting enzymes in LGQ-17::3*acb* led to the accumulation of a large number of intermediates or shunt products, which affected its growth and resulted in a significant decrease in acarbose production. Therefore, identifying the rate-limiting enzymes in strain LGQ-17::3*acb* is expected to alleviate the bottlenecks in acarbose production.

In LGQ-17::3*acb,* since all *attB*$^{\Phi C31}$ sites were occupied and the apramycin resistance gene *aac(3)IV* was integrated into the genome, a new integration system was needed to introduce additional genetic elements. Therefore, the *aac(3)IV* in pRT801 was replaced with the streptomycin resistance gene *SmR,* resulting in the construction of plasmid pRT801-*str*, which contains the ΦBT1 attachment site and the streptomycin resistance gene (Figure S13). Due to the essential requirement of AcbC, M, O, N, J, V, I, and S in acarbose biosynthesis—responsible for the C_7-cyclitol moiety, amino-deoxyhexose moiety, and the condensation reaction,[22] they were individually overexpressed, under the control of the *kasOp** promoter, in LGQ-17::3*acb* in an attempt to reverse the acarbose biosynthesis capacity. The construction and verification of pRT801-*str*-derived integrated vectors and corresponding engineered strains are shown in Figure S14. Using the integrated vector pRT801-*str*, mutant LGQ-17::3*acb*::pRT801-*str* was created as a control strain.

Fermentation analysis showed that overexpression of *acbJ* and *acbS* in LGQ-17::3*acb* led to a production boost, with the acarbose titer increasing by 1.04-fold and 98%, respectively, and exhibited no significant growth difference compared with LGQ-17::3*acb*::pRT801-*str* (Figure 4). Overexpression of *acbN* in LGQ-17::3*acb* did not result in significant changes in acarbose production and biomass. However, the engineered strains LGQ-17::3*acb*::*kasOp**-*acbC*, *acbM*, *acbO*, *acbV*, and *acbI* showed a 14.4% to 74.4% decrease in acarbose titer, but a 4.0% to 30.4% increase in biomass compared with the control strain LGQ-17::3*acb*::pRT801-*str*.

The productivity of LGQ-17::3*acb*::*kasOp**-*acbS* and LGQ-17::3*acb*::*kasOp**-*acbJ* is 0.56 and 0.53, respectively, both of which exceed the three-copy *acb* strain LGQ-14::2*acb*. Since the overexpression of *acbJ* in LGQ-17::3*acb* showed the most significant increase in acarbose production, we reasoned that overexpressing different doses of *acbJ* might further enhance the acarbose titer. Therefore, besides the *kasOp** promoter, *acbJ* was overexpressed under the control of a weaker *ermEp** promoter and a stronger *stnYp* promoter,[37] resulting in the construction of the engineered strains LGQ-17::3*acb*::*ermEp**-*acbJ* and LGQ-17::3*acb*::*stnYp-acbJ* (Figure S14). As shown in Figure S15, increasing promoter strength led to a slight boost in acarbose production. The acarbose titer of LGQ-17::3*acb*::*stnYp-acbJ* increased by 1.08-fold (6.31 g/L) compared with the control strain LGQ-17::3*acb*::pRT801-*str* and its productivity reached 0.58.

3.5. Optimization of a Fed-Batch Fermentation Procedure. To assess the potential of the engineered strain LGQ-17::3*acb*::*stnYp-acbJ*, fed-batch fermentation was conducted in baffled flasks. It has been shown that supplementing glucose, maltose, and nitrogen sources increases the production of acarbose during fermentation. In addition, glucose plays a key role in acarbose production during fermentation, especially when considering the timing and amount of glucose fed.[11,25] Therefore, we first tested the effect of different glucose-supplementation strategies and supplementation times on acarbose titer. As shown in Figures S16 andS17, a total glucose supplementation of 6% (w/v, day 1−6, 1% per day) showed the most significant increase in acarbose titer. However, after 6 days of glucose supplementation, the acarbose titer decreased across all experimental groups. Consequently, we concluded that the optimal glucose-supplementing strategy for LGQ-17::3*acb*::*stnYp-acbJ* was to supplement 1% glucose for days 1−5.

Subsequently, to evaluate the effect of supplementing maltose and a complex nitrogen source (CNS, including soy flour, yeast, and glutamate) on acarbose titer for LGQ-17::3*acb*::*stnYp-acbJ*, we tested the supplementation of different concentrations of glucose (group A), glucose and maltose

https://doi.org/10.1021/acs.jafc.5c00613
J. Agric. Food Chem. 2025, 73, 12845−12855

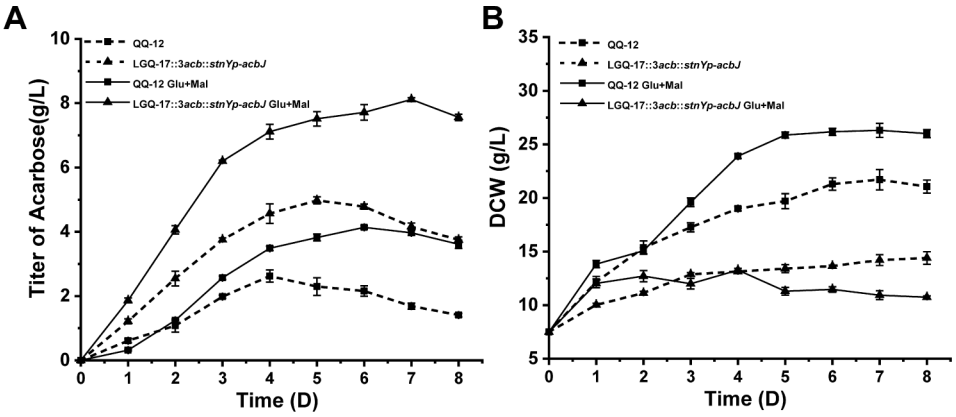

Figure 5. The fed-batch fermentation of the engineered strain LGQ-17::3*acb*::*stnYp-acbJ*. The titer of acarbose (A) and the dry cell weight (B) of LGQ-17::3*acb*::*stnYp-acbJ*. QQ-12 was the control strain. The fermentation was continued for 8 days, and 0.5 g of glucose and 0.17 g of maltose were added on 24, 48, 72, 96, and 120 h. Error bars, mean ± SD (n = 3 biological replicates).

(groups B, C, D, E), or glucose, maltose, and a complex nitrogen source (groups F, G, H) over an 8-day fermentation period (Figure S18A). As shown in Figure S18B,C, for all groups, the highest acarbose titers appeared in day 7. The highest titer of acarbose in shake flasks, 8.12 g/L, representing a 1.1-fold increase, was obtained in group D (1% glucose and 0.67% maltose, days 1−5). However, an 8.6% decrease in biomass occurred when compared with that of the control strain QQ-12 (Figure 5). Under the same fed-batch fermentation conditions, LGQ-17::3*acb*::*stnYp-acbJ* showed a 32.9% increase in acarbose titer (4.52 g/L) and a 61.2% decrease in biomass compared to QQ-12 in a 3 L bioreactor. Besides, the supplementation of glucose and maltose facilitated the prolongation of fermentation time and increased the yield of acarbose for LGQ-17::3*acb*::*stnYp-acbJ* and QQ-12. This confirms the important role of glucose and maltose in acarbose fermentation in *Actinoplanes* sp..

4. DISCUSSION

Iterative metabolic engineering modifications require a basic toolkit for genetic engineering in *Actinoplanes* sp. SE50/110. In this study, we expanded the integration sites and antibiotic resistance spectra for genes or intact BGC overexpression in *Actinoplanes* sp.. The recipient cells for conjugation of *Actinoplanes* sp. could be the mycelia or spores for the ΦC31-derived integrative plasmid pSET152. However, the conjugation efficiency with mycelia as the recipient cells was 89-fold higher than with spores.[12,14] We also demonstrated that conjugation efficiency using mycelia as recipient cells is higher than using spores for the ΦBT1-derived integrative plasmid pRT801, and the conjugation efficiency with the mycelia as the recipient cells was 25-fold higher than with spores as the recipient cells.[12] Integration sites for TG1, R4, and pSAM2 were identified as being capable of efficient conjugation in the *Actinoplanes* sp. for the first time (Table 1). Among them, R4 demonstrated a conjugation efficiency as high as 24.4% and was neutral concerning acarbose biosynthesis and strain growth (Figure 1), making it an excellent integration site for genetic manipulations of *Actinoplanes* sp.. Additionally, we predicted other integration sites, such as ΦJoe and μ1/6, which showed high sequence identity and could serve as candidate bacteriophage Att/Int sites for *Actinoplanes* sp. (Table S3). Mapping of these SSR sites in *Actinoplanes* sp. SE50/110 is shown in Figure S4.

We found that the ΦC31-based integration plasmid pSET152 led to a decrease in both acarbose production and strain growth, similar to results reported in previous studies. The $attB^{\Phi C31}$ site is located within the gene *ACPL_6602* (coding for a pirin-like protein).[12] Although the function of this protein in bacteria is poorly understood, it is crucial and affects various biological processes.[38] The inactivation of the pirin-like protein due to the pSET152 insertion likely leads to a decrease in the biomass of QQ-2, which in turn reduces the acarbose titer decrease (Figure 1). Streptomycin is an aminoglycoside antibiotic produced by the fermentation of *Streptomyces griseus*.[39] As a widely used resistance selection marker, the working concentration of streptomycin is approximately 50 mg/L.[33] Unexpectedly, in *Actinoplanes* sp., the optimal working concentration of streptomycin is extremely low, at just 0.1 mg/L.

During the construction of multicopy *acb* strains, 12 individual exconjugants were selected for each mutant to calculate integration efficiency. As shown in Figure S12A, pLQ666 (52.3 kb) and pSET152 (5.7 kb) were integrated into the native $attB^{\Phi C31}$ site in LGQ-4, demonstrating an insertion efficiency of 100% (12/12). For LGQ-14::2*acb* and LGQ-14::2pSET152 (Figure S12B), pLQ666 and pSET152 were integrated into the native $attB^{\Phi C31}$ site in LGQ-14 with nearly 100% efficiency (12/12) and with 75% efficiency (8/12) into the artificial $attB^{\Phi C31}$ site RE10-*attB*. Thus, the efficiency of integrating two copies of the plasmid simultaneously is 75% for both pLQ666 and pSET152 by one round of conjugal transfer. Furthermore, for LGQ-17::3*acb* and LGQ-17::3pSET152 (Figure S12C), pLQ666 and pSET152 were integrated into the native $attB^{\Phi C31}$ and artificial $attB^{\Phi C31}$ site RE2-*attB* in LGQ-17 with nearly 100% efficiency (12/12). However, the efficiency of integration into the artificial $attB^{\Phi C31}$ site RE10-*attB* was 41.7% (5/12) and 58.3% (7/12), respectively. Thus, for pLQ666 and pSET152, the efficiency of integrating three plasmids simultaneously is 41.7% and 58.3% by one round of conjugation, respectively. These results indicate that the size of the integrated plasmids does not affect integration efficiency in *Actinoplanes* sp., but the efficiency decreases as the number of integrated plasmids increases. The position of $attB^{\Phi C31}$ in the genome significantly influences integration efficiency.[40,41]

Using MSGE, engineered strains containing one to four *acb*s were obtained after one round of conjugal transfer in the QQ-12 strain and exhibited a significant improvement in acarbose

https://doi.org/10.1021/acs.jafc.5c00613
J. Agric. Food Chem. 2025, 73, 12845−12855

production (Figure 3). Unexpectedly, the biomass of these engineered strains gradually decreased along with an increasing number of *acb*, with the four-*acb*s strain LGQ-17::3*acb* showing a 37.6% decrease in its biomass. It is critical to regulate intracellular phosphorylated metabolite levels because high levels can cause toxic effects on cells, leading to DNA damage and growth inhibition.[42] During acarbose synthesis in *Actinoplanes* sp. SE50/110, the C_7-cyclitol intermediates predominantly exist in the form of phosphorylated metabolites. Excess accumulation of these phosphorylated C_7-cyclitol intermediates may be toxic and cause growth inhibition.[21] We measured the concentrations of endogenous 1-*epi*-valienol-7-P and valienol-7-P in multicopy *acb*s-engineered strains. As shown in Figure S19A, compared with QQ-12::pSET152, strains LGQ-4::*acb*, LGQ-14::2*acb*, and LGQ-17::3*acb* exhibited a 0.89-fold, 2.0-fold, and 4.3-fold increase in the total amount of 1-*epi*-valienol-7-P and valienol-7-P, respectively. These results indicate that as the copy number of *acb*s increases, there is a substantial accumulation of intracellular phosphorylated C_7-cyclitol intermediates 1-*epi*-valienol-7-P and valienol-7-P, leading to decreased strain growth. However, the toxic effects of these phosphorylated intermediates on cells need to be tested by further experiments. For example, when these compounds are fed in vitro, their effect on bacterial biomass will appear. Afterward, the growth inhibition of the bacteria will be alleviated by resolving the mechanism of toxic effects.

Although the multicopy BGC strategy was effective in enhancing acarbose production, we found that the acarbose production titer of the four-copy strains was substantially reduced compared with the three-copy strains. It has been reported that the dephosphorylation of phosphorylated intermediates 1-*epi*-valienol-7-P and valienol-7-P, leading to the accumulation of shunt products 1-*epi*-valienol and valienol, is part of a detoxification process in *Actinoplanes* sp..[21] Therefore, we measured the levels of shunt products in multicopy strains. Fermentation analysis showed that strains LGQ-4::*acb*, LGQ-14::2*acb*, and LGQ-17::3*acb* exhibited a 74.0%, 123%, and 45.5% increase in the total amount of 1-*epi*-valienol and valienol, respectively, compared with QQ-12::pSET152. However, LGQ-17::3*acb* showed a 34.7% decrease in the total amount of 1-*epi*-valienol and valienol compared with LGQ-14::2*acb* (Figure S19B), suggesting an insufficient detoxification capacity of LGQ-17::3*acb*. AcbJ not only catalyzes the formation of 1-P-valienol from valienol-1,7-diP, which is involved in acarbose synthesis,[22] but also facilitates the dephosphorylation of 1-*epi*-valienol-7-P, valienone-7-P, and valienol-7-P to produce shunt products.[21] Additionally, the transcription of *acbJ* in LGQ-17::3*acb* was 56.8% lower compared with LGQ-14::2*acb* (Figure S20), suggesting that AcbJ might be the rate-limiting enzyme in LGQ-17::3*acb*. Consequently, among all candidate rate-limiting enzymes, the overexpression of *acbJ* resulted in significantly enhanced acarbose production, reversing the acarbose production capacity of LGQ-17::3*acb*. Overexpression of *acbJ* in LGQ-17::3*acb* resulted in the formation of more shunt products, 1-*epi*-valienol and valienol (twice as high as in LGQ-17::3*acb*, Figure S21), which might also increase the utilization of valienol-1,7-diP and reduce intracellular accumulation, thereby increasing the titer of acarbose.

During fermentation, the addition of various concentrations of glucose, maltose, and nitrogen sources has been shown to maintain cell growth and improve the titer of acarbose,[11,21,25] To further enhance the acarbose titer of the best engineered strain, LGQ-17::3*acb*::*stnYp-acbJ*, we optimized the addition of glucose, maltose, and organic nitrogen sources to achieve more suitable cultivation conditions. Fed-batch fermentation allows for prolonged fermentation times and improved acarbose titer in LGQ-17::3*acb*::*stnYp-acbJ* (Figures S16−S18 and5). After optimizing the fed-batch fermentation, the engineered strain LGQ-17::3*acb*::*stnYp-acbJ* produced 8.12 g/L of acarbose on day 7 in shake flasks (Figure 5), whose acarbose titer had a 51% improvement than batch fermentation (5.38 g, Figure S16). Subsequently, we assessed the scale-up feasibility of LGQ-17::3*acb*::*stnYp-acbJ* through fed-batch fermentation in a 3-L bioreactor. The results showed that the engineered strain LGQ-17::3*acb*::*stnYp-acbJ* produced 4.52 g/L of acarbose in 7 days, representing a 33% titer improvement of acarbose when compared with the control strain QQ-12 (Figure S22). To investigate the discrepancy of acarbose titer between bioreactors and shake flasks, first, the titer of shunt products of the engineered strain LGQ-17::3*acb*::*stnYp-acbJ* in both cultivation systems was analyzed. Strain LGQ-17::3*acb*::*stnYp-acbJ* exhibited a significant decrease in shunt products 1-*epi*-valienol and valienol in bioreactors (Figure S23A), consistent with the trend of acarbose titer. This indicated that the reduced acarbose titer under bioreactor conditions could not be attributed to a substantial loss of shunt products. Subsequently, transcript levels of the *acb* gene cluster were compared between bioreactor and shake flask cultures. Strain LGQ-17::3*acb*::*stnYp-acbJ* did not have a higher level of transcription of the *acb* gene cluster in the bioreactor than in shake flask fermentation (Figure S23B). This result suggests that the decrease in acarbose titer in the bioreactor is not due to low gene transcription levels. It is possible that the destruction of the mycelium by vigorous agitation of the stirring paddles is responsible for the decrease in acarbose production in the bioreactor. And it will be possible to solve this problem by optimizing the process for strain LGQ-17::3*acb*::*stnYp-acbJ* in the bioreactor. Besides, if the accumulation of toxic phosphorylated intermediates of LGQ-17::3*acb*::*stnYp-acbJ* could be effectively reduced, allowing for the restoration of cell growth, then acarbose production would be substantially increased in the bioreactor. The optimized fed-batch greatly enhanced the production capacity of strain LGQ-17::3*acb*::*stnYp-acbJ*. And this can also provide detailed and precise fermentation parameters for the industrial scale-up production of acarbose.

In conclusion, we have expanded the genetic toolkit for iterative metabolic engineering in *Actinoplanes* sp., including Att/Int systems and resistance screening markers. Using MSGE, multicopy *acb*s were integrated into *Actinoplanes* sp., resulting in significant increases in acarbose titer. Furthermore, by overexpressing the rate-limiting enzyme AcbJ, the acarbose production capacity of the four-copy strain was improved. Optimization of fed-batch fermentation further increased the acarbose yield in the engineered strain. The engineered strain LGQ-17::3*acb*::*stnYp-acbJ* shows strong potential for industrial application, which would boost the acarbose production capacity of *Actinoplanes* sp. and significantly reduce the cost of drug production. However, there are still major challenges in scaling up production. Our study demonstrates the great potential of modifying *Actinoplanes* sp. to increase acarbose production by metabolic engineering. Subsequent studies will focus on reducing shunt products, alleviating toxic effects, and achieving industrial scale-up.

https://doi.org/10.1021/acs.jafc.5c00613
J. Agric. Food Chem. 2025, 73, 12845−12855

■ ASSOCIATED CONTENT

Supporting Information

The Supporting Information is available free of charge at https://pubs.acs.org/doi/10.1021/acs.jafc.5c00613.

Plasmids and strains (Table S1); primers and oligonucleotide sequences (Table S2); site-specific integration systems (Table S3, Figure S4); antibiotics concentrations tests (Table S4−S5); verification of the mutants (Figure S1−S3, S5−S12, S14); verification of the vector pRT801-*str* (Figure S13); the titer of acarbose and dry cell weight (Figure S15−S18, S22); endogenous 1-*epi*-valienol-7-P and valienol-7-P and shunt products 1-*epi*-valienol and valienol (Figure S19, S21); and transcriptional analysis (Figure S23) (PDF)

■ AUTHOR INFORMATION

Corresponding Author

Linquan Bai − *State Key Laboratory of Microbial Metabolism, School of Life Sciences and Biotechnology, Shanghai Jiao Tong University, Shanghai 200240, China; College of Life Science, Tarim University, Alar 843300, China;* orcid.org/0000-0002-3269-9747; Email: bailq@sjtu.edu.cn

Authors

Guoqiang Liu − *State Key Laboratory of Microbial Metabolism, School of Life Sciences and Biotechnology, Shanghai Jiao Tong University, Shanghai 200240, China*

Qi Liu − *State Key Laboratory of Microbial Metabolism, School of Life Sciences and Biotechnology, Shanghai Jiao Tong University, Shanghai 200240, China*

Xiaotong Song − *State Key Laboratory of Microbial Metabolism, School of Life Sciences and Biotechnology, Shanghai Jiao Tong University, Shanghai 200240, China*

Xingzhi Jiao − *State Key Laboratory of Microbial Metabolism, School of Life Sciences and Biotechnology, Shanghai Jiao Tong University, Shanghai 200240, China*

Wanping Zhou − *State Key Laboratory of Microbial Metabolism, School of Life Sciences and Biotechnology, Shanghai Jiao Tong University, Shanghai 200240, China*

Qianjin Kang − *State Key Laboratory of Microbial Metabolism, School of Life Sciences and Biotechnology, Shanghai Jiao Tong University, Shanghai 200240, China; College of Life Science, Tarim University, Alar 843300, China;* orcid.org/0000-0002-4894-0056

Complete contact information is available at: https://pubs.acs.org/10.1021/acs.jafc.5c00613

Funding

This work was financially supported by the Shanghai Municipal Science and Technology Major Project, the Shanghai Committee of Science and Technology (Grant No. 24HC2810200), and the National Natural Science Foundation of China (Grant No. 31830104) to L.B.

Notes

The authors declare no competing financial interest.

■ ACKNOWLEDGMENTS

The authors are grateful to Prof. Shuangjun Lin, Prof. Lei Li, and Yudian Yu from Shanghai Jiao Tong University for kindly providing the plasmids pSET-*stnYp-indC*, pRT801, pTG1, pLR4, and ppM927-*xis*. They also thank Dr. Wei Zhang from the Core Facility and Technical Service Center for the School of Life Sciences and Biotechnology, SJTU, for help with LC-Q-TOFMS/MS data acquisition and data analysis.

■ REFERENCES

(1) Wehmeier, U. F.; Piepersberg, W. Biotechnology and Molecular Biology of the α-Glucosidase Inhibitor Acarbose. *Appl. Microbiol. Biotechnol.* **2004**, *63* (6), 613−625.

(2) Dianna, J.; Magliano, E. J. B. IDF DIABETES ATLAS. *IDF Diabetes Atlas 10th Edition Scientific Committee*; Diabetes Atlas, 2021.

(3) Gu, Y.; Wang, X.; Li, J.; Zhang, Y.; Zhong, H.; Liu, R.; Zhang, D.; Feng, Q.; Xie, X.; Hong, J.; et al. Analyses of Gut Microbiota and Plasma Bile Acids Enable Stratification of Patients for Antidiabetic Treatment. *Nat. Commun.* **2017**, *8* (1), 1785.

(4) Martin, A. M.; Yabut, J. M.; Choo, J. M.; Page, A. J.; Sun, E. W.; Jessup, C. F.; Wesselingh, S. L.; Khan, W.I.; Rogers, G.B.; Steinberg, G. R.; et al. The Gut Microbiome Regulates Host Glucose Homeostasis via Peripheral Serotonin. *Proc. Natl. Acad. Sci. U. S. A.* **2019**, *116* (40), 19802−19804.

(5) Tsunoda, T.; Asamizu, S.; Mahmud, T. Biochemical Characterization of GacI, a Bifunctional Glycosyltransferase-Phosphatase Enzyme Involved in Acarbose Biosynthesis in *Streptomyces glaucescens* GLA.O. *Biochemistry* **2022**, *61* (22), 2628−2635.

(6) Tanoeyadi, S.; Tsunoda, T.; Ito, T.; Philmus, B.; Mahmud, T. Acarbose May Function as a Competitive Exclusion Agent for the Producing Bacteria. *ACS Chem. Biol.* **2023**, *18* (2), 367−376.

(7) Ren, F.; Chen, L.; Tong, Q. Highly Improved Acarbose Production of Actinomyces through the Combination of ARTP and Penicillin Susceptible Mutant Screening. *World J. Microbiol. Biotechnol.* **2017**, *33* (1), 16.

(8) Wei, S. J.; Cheng, X.; Huang, L.; Li, K. T. Medium Optimization for Acarbose Production by *Actinoplanes sp*. A56 Using the Response Surface Methodology. *African J. Biotechnol.* **2010**, *9* (13), 1949−1954.

(9) Cheng, X.; Peng, W. F.; Huang, L.; Zhang, B.; Li, K. T. A Novel Osmolality-Shift Fermentation Strategy for Improving Acarbose Production and Concurrently Reducing Byproduct Component C Formation by *Actinoplanes sp*. A56. *J. Ind. Microbiol. Biotechnol.* **2014**, *41* (12), 1817−1821.

(10) Wang, Y. J.; Liu, L. L.; Feng, Z. H.; Liu, Z. Q.; Zheng, Y. G. Optimization of Media Composition and Culture Conditions for Acarbose Production by *Actinoplanes utahensis* ZJB-08196. *World J. Microbiol. Biotechnol.* **2011**, *27* (12), 2759−2766.

(11) Wang, Y. J.; Liu, L. L.; Wang, Y. S.; Xue, Y. P.; Zheng, Y. G.; Shen, Y. C. *Actinoplanes utahensis* ZJB-08196 Fed-Batch Fermentation at Elevated Osmolality for Enhancing Acarbose Production. *Bioresour. Technol.* **2012**, *103* (1), 337−342.

(12) Gren, T.; Ortseifen, V.; Wibberg, D.; Schneiker-Bekel, S.; Bednarz, H.; Niehaus, K.; Zemke, T.; Persicke, M.; Pühler, A.; Kalinowski, J. Genetic Engineering in *Actinoplanes sp*. SE50/110 − Development of an Intergeneric Conjugation System for the Introduction of Actinophage-Based Integrative Vectors. *J. Biotechnol.* **2016**, *232*, 79−88.

(13) Wolf, T.; Gren, T.; Thieme, E.; Wibberg, D.; Zemke, T.; Pühler, A.; Kalinowski, J. Targeted Genome Editing in the Rare Actinomycete *Actinoplanes sp*. SE50/110 by Using the CRIPSR/Cas9 System. *J. Biotechnol.* **2016**, *231*, 122−128.

(14) Zhao, Q.; Xie, H.; Peng, Y.; Wang, X.; Bai, L. Improving Acarbose Production and Eliminating the by-Product Component C with an Efficient Genetic Manipulation System of *Actinoplanes sp*. SE50/110. *Synth. Syst. Biotechnol.* **2017**, *2* (4), 302−309.

(15) Wolf, T.; Schneiker-Bekel, S.; Neshat, A.; Ortseifen, V.; Wibberg, D.; Zemke, T.; Pühler, A.; Kalinowski, J. Genome Improvement of the Acarbose Producer *Actinoplanes sp*. SE50/110 and Annotation Refinement Based on RNA-Seq Analysis. *J. Biotechnol.* **2017**, *251* (December 2016), 112−123.

(16) Wendler, S.; Otto, A.; Ortseifen, V.; Bonn, F.; Neshat, A.; Schneiker-Bekel, S.; Wolf, T.; Zemke, T.; Wehmeier, U. F.; Hecker, M.; et al. Comparative Proteome Analysis of *Actinoplanes sp*. SE50/

110 Grown with Maltose or Glucose Shows Minor Differences for Acarbose Biosynthesis Proteins but Major Differences for Saccharide Transporters. *J. Proteomics* **2016**, *131*, 140−148.
(17) Droste, J.; Ortseifen, V.; Schaffert, L.; Persicke, M.; Schneiker-Bekel, S.; Pühler, A.; Kalinowski, J. The Expression of the Acarbose Biosynthesis Gene Cluster in *Actinoplanes sp*. SE50/110 Is Dependent on the Growth Phase. *BMC Genomics* **2020**, *21* (1), 818.
(18) Wang, Y.; Wu, J. Reconstruction and in Silico Analysis of an *Actinoplanes sp*. SE50/110 Genome-Scale Metabolic Model for Acarbose Production. *Front. Microbiol.* **2015**, *6* (JUN), 632.
(19) Droste, J.; Kulisch, M.; Wolf, T.; Schaffert, L.; Schneiker-Bekel, S.; Pühler, A.; Kalinowski, J. A Maltose-Regulated Large Genomic Region Is Activated by the Transcriptional Regulator MalT in *Actinoplanes sp*. SE50/110. *Appl. Microbiol. Biotechnol.* **2020**, *104* (21), 9283−9294.
(20) Schaffert, L.; März, C.; Burkhardt, L.; Droste, J.; Brandt, D.; Busche, T.; Rosen, W.; Schneiker-Bekel, S.; Persicke, M.; Pühler, A.; et al. Evaluation of Vector Systems and Promoters for Overexpression of the Acarbose Biosynthesis Gene AcbC in *Actinoplanes sp*. SE50/110. *Microb. Cell Fact.* **2019**, *18* (1), 114.
(21) Zhao, Q.; Luo, Y.; Zhang, X.; Kang, Q.; Zhang, D.; Zhang, L.; Bai, L.; Deng, Z. A Severe Leakage of Intermediates to Shunt Products in Acarbose Biosynthesis. *Nat. Commun.* **2020**, *11* (1), 1468.
(22) Tsunoda, T.; Samadi, A.; Burade, S.; Mahmud, T. Complete Biosynthetic Pathway to the Antidiabetic Drug Acarbose. *Nat. Commun.* **2022**, *13* (1), 3455.
(23) Xie, H.; Zhao, Q.; Zhang, X.; Kang, Q.; Bai, L. Comparative Functional Genomics of the Acarbose Producers Reveals Potential Targets for Metabolic Engineering. *Synth. Syst. Biotechnol.* **2019**, *4* (1), 49−56.
(24) Schaffert, L.; Schneiker-Bekel, S.; Gierhake, J.; Droste, J.; Persicke, M.; Rosen, W.; Pühler, A.; Kalinowski, J. Absence of the Highly Expressed Small Carbohydrate-Binding Protein Cgt Improves the Acarbose Formation in *Actinoplanes sp*. SE50/110. *Appl. Microbiol. Biotechnol.* **2020**, *104* (12), 5395−5408.
(25) Li, Z.; Yang, S.; Zhang, Z.; Wu, Y.; Tang, J.; Wang, L.; Chen, S. Enhancement of acarbose production by genetic engineering and fed-batch fermentation strategy in Actinoplanes sp. SIPI12-34. *Microb. Cell Fact.* **2022**, *21* (1), 240.
(26) Palazzotto, E.; Tong, Y.; Lee, S. Y.; Weber, T. Synthetic Biology and Metabolic Engineering of Actinomycetes for Natural Product Discovery. *Biotechnol. Adv.* **2019**, *37* (6), 107366.
(27) Shi, S.; Liang, Y.; Zhang, M. M.; Ang, E. L.; Zhao, H. A Highly Efficient Single-Step, Markerless Strategy for Multi-Copy Chromosomal Integration of Large Biochemical Pathways in *Saccharomyces cerevisiae*. *Metab. Eng.* **2016**, *33*, 19−27.
(28) Baltz, R. H. Genetic Manipulation of Secondary Metabolite Biosynthesis for Improved Production in *Streptomyces* and Other Actinomycetes. *J. Ind. Microbiol. Biotechnol.* **2016**, *43* (2−3), 343−370.
(29) Kormanec, J.; Rezuchova, B.; Homerova, D.; Csolleiova, D.; Sevcikova, B.; Novakova, R.; Feckova, L. Recent Achievements in the Generation of Stable Genome Alterations/Mutations in Species of the Genus *Streptomyces*. *Appl. Microbiol. Biotechnol.* **2019**, *103* (14), 5463−5482.
(30) Haginaka, K.; Asamizu, S.; Ozaki, T.; Igarashi, Y.; Furumai, T.; Onaka, H. Genetic Approaches to Generate Hyper-Producing Strains of Goadsporin: The Relationships between Productivity and Gene Duplication in Secondary Metabolite Biosynthesis. *Biosci., Biotechnol., Biochem.* **2014**, *78* (3), 394−399.
(31) Li, L.; Zheng, G.; Chen, J.; Ge, M.; Jiang, W.; Lu, Y. Multiplexed Site-Specific Genome Engineering for Overproducing Bioactive Secondary Metabolites in Actinomycetes. *Metab. Eng.* **2017**, *40* (December 2016), 80−92.
(32) Li, L.; Wei, K.; Liu, X.; Wu, Y.; Zheng, G.; Chen, S.; Jiang, W.; Lu, Y. aMSGE: Advanced Multiplex Site-Specific Genome Engineering with Orthogonal Modular Recombinases in Actinomycetes. *Metab. Eng.* **2019**, *52* (October 2018), 153−167.
(33) Gust, B.; Kieser, T.; Chater, K. *PCR Targeting System in Streptomyces coelicolor A3(2)*; John Innes Centre, 2000, pp. 1−39.
(34) Baltz, R. H. Streptomyces Temperate Bacteriophage Integration Systems for Stable Genetic Engineering of Actinomycetes (and Other Organisms). *J. Ind. Microbiol. Biotechnol.* **2012**, *39* (5), 661−672.
(35) Blin, K.; Shaw, S.; Kloosterman, A. M.; Charlop-Powers, Z.; Van Wezel, G. P.; Medema, M. H.; Weber, T. AntiSMASH 6.0: Improving Cluster Detection and Comparison Capabilities. *Nucleic Acids Res.* **2021**, *49* (W1), W29−W35.
(36) Li, L.; Liu, X.; Jiang, W.; Lu, Y. Recent Advances in Synthetic Biology Approaches to Optimize Production of Bioactive Natural Products in Actinobacteria. *Front. Microbiol.* **2019**, *10* (November), 2467.
(37) Guo, W.; Xiao, Z.; Huang, T.; Zhang, K.; Pan, H. X.; Tang, G. L.; Deng, Z.; Liang, R.; Lin, S. Identification and Characterization of a Strong Constitutive Promoter *stnYp* for Activating Biosynthetic Genes and Producing Natural Products in *Streptomyces*. *Microb. Cell Fact.* **2023**, *22* (1), 127.
(38) Talà, A.; Damiano, F.; Gallo, G.; Pinatel, E.; Calcagnile, M.; Testini, M.; Fico, D.; Rizzo, D.; Sutera, A.; Renzone, G.; et al. Pirin: A Novel Redox-Sensitive Modulator of Primary and Secondary Metabolism in *Streptomyces*. *Metab. Eng.* **2018**, *48* (January), 254−268.
(39) Webster, C. M.; Shepherd, M. A Mini-Review: Environmental and Metabolic Factors Affecting Aminoglycoside Efficacy. *World J. Microbiol. Biotechnol.* **2023**, *39* (1), 7.
(40) Deng, L.; Zhao, Z.; Liu, L.; Zhong, Z.; Xie, W.; Zhou, F.; Xu, W.; Zhang, Y.; Deng, Z. S. Y.; Sun, Y. Dissection of 3D Chromosome Organization in *Streptomyces coelicolor* A3(2) Leads to Biosynthetic Gene Cluster Overexpression. *Proc. Natl. Acad. Sci. U. S. A.* **2023**, *120* (11), No. e2222045120.
(41) Bilyk, B.; Horbal, L.; Luzhetskyy, A. Chromosomal Position Effect Influences the Heterologous Expression of Genes and Biosynthetic Gene Clusters in *Streptomyces albus* J1074. *Microb. Cell Fact.* **2017**, *16* (1), 5.
(42) Kuznetsova, E.; Nocek, B.; Brown, G.; Makarova, K. S.; Flick, R.; Wolf, Y. I.; Khusnutdinova, A.; Evdokimova, E.; Jin, K.; Tan, K.; Hanson, A. D.; Hasnain, G.; Zallot, R.; De Crécy-Lagard, V.; Babu, M.; Savchenko, A.; Joachimiak, A.; Edwards, A. M.; Koonin, E. V.; Yakunin, A. F. Functional Diversity of Haloacid Dehalogenase Superfamily Phosphatases from *Saccharomyces cerevisiae*: Biochemical, Structural, and Evolutionary Insights. *J. Biol. Chem.* **2015**, *290* (30), 18678−18698.

https://doi.org/10.1021/acs.jafc.5c00613
J. Agric. Food Chem. 2025, 73, 12845−12855